

# Raman and Polarization-sensitive digital holographic imaging for rapid and label-free prostate cancer diagnosis

Hossein Khadem<sup>1</sup>, Maria Antonietta Ferrara<sup>2</sup>, Maria Mangini<sup>1</sup>, Alberto Luini<sup>1</sup>, Giuseppe Coppola<sup>2,†,\*</sup>, Anna Chiara De Luca<sup>1,†,\*</sup>

<sup>1</sup>Institute for the Experimental Endocrinology and Oncology “G. Salvatore”, Secondary Unit, National Research Council, Naples, Italy

<sup>2</sup>Institute of Applied Sciences and Intelligent Systems, National Research Council, Naples, Italy

**Abstract.** In this study, we report the results of two non-invasive optical methods, Raman microscopy (RM) and polarization-sensitive digital holographic imaging (PSDHI), for distinguishing prostate cancer cells from healthy ones. RM reveals cancer cells metabolize glucose faster, storing it as fatty acids and cholesteryl esters in lipid droplets (LDs). On the other hand, PSDHI shows significant morphological changes in LDs in glucose-incubated cancer cells, including number, volume, and refractive index. High birefringence in cancer LDs under perpendicular polarizations was observed, enabling fast discrimination with over 90% accuracy. PSDHI results align closely with Raman microscopy, suggesting its potential as a promising, high-speed technique for cancer screening purposes.

## 1 Introduction

Prostate cancer is the most common cancer among men and the second leading cause of cancer-related deaths in men [1]. Early prostate cancer diagnosis can aid successful treatment [2].

Raman microscopy (RM), as a non-invasive method, provide molecular information, but it is time-consuming and unsuitable for screening [3]. Polarization-sensitive digital holographic imaging (PSDHI) report quantitative data on morphology, refractive index, and birefringence rapidly [4,5]. Combining these two offers a full picture of cellular composition, potentially leading to highly accurate cancer detection [6].

Cancer cells have up to 10 times higher uptake of glucose (Glc) compared to healthy ones [7]. This can serve as a fundamental strategy for detecting cancer cells. For RM, it is preferable to use deuterated glucose (deut-Glc) with C–D bonds instead C–H. The Raman band of C–D is located in the Raman silent region, enabling the tracking of glucose with high contrast. Additionally, deuterated glucose follows the same metabolic pathway as normal glucose, being metabolized by the cell and stored in lipid droplets.

Here, we use RM and PSDHI to study lipid droplets (LDs) in PNT2 and PC3 cells as prostate healthy and cancer cells, respectively. RM results indicate that cancer cells store Glc as fatty acids and cholesteryl esters in LDs. On the other hand, PSDHI results show that LDs in cancer cells have a high birefringence, useful for discrimination. PSDHI results show an accuracy of over 90%, aligned well with RM, suggesting PSDHI as a high-speed and label-free technique for screening.

## 2 Materials and methods

PNT2 and PC3 cells were plated on CaF<sub>2</sub> coverslips. Cells were cultured for 1 h without Glc or a specific time in a medium containing 25 mM deut-Glc, fresh medium was added every 24 h [8].

A schematic of the RM setup is shown in Fig. 1(a). Laser power on the sample was 2 mW, and Raman spectra were acquired with a 1 s integration time.

Figure 2 depicts the experimental setup of PSDHI. The laser light is split into two beams of equal intensity, referred to as the object beam and the reference beam, by a beam splitter (BS). The reference beam is split into two beams with orthogonal polarizations and equal intensities by a polarization beam splitter (PBS). Half-wave plates (HWP) number 1 and 2 determine the polarization of these beams to be either along the horizontal or vertical components of the object beam. On the other hand, HWP 3 determines the polarization of the object beam to have horizontal and vertical components with equal intensities. The acquisition time for all images was 0.4 s.

## 3 Results and discussion

Figure 1(b) (top) illustrates a Raman image constructed based on the Raman intensity of corresponding peaks for protein (red), C–D (green), and DNA (blue). As evident, the intensity distribution of the 2120 cm<sup>-1</sup> peak corresponding to the C–D vibration is only observed in circular areas with a diameter of approximately 1 to 2 micrometers present in the perinuclear region of the cell.

\* Corresponding authors: [giuseppe.coppola@cnr.it](mailto:giuseppe.coppola@cnr.it); [annachiara.deluca@cnr.it](mailto:annachiara.deluca@cnr.it)

† These authors contributed equally

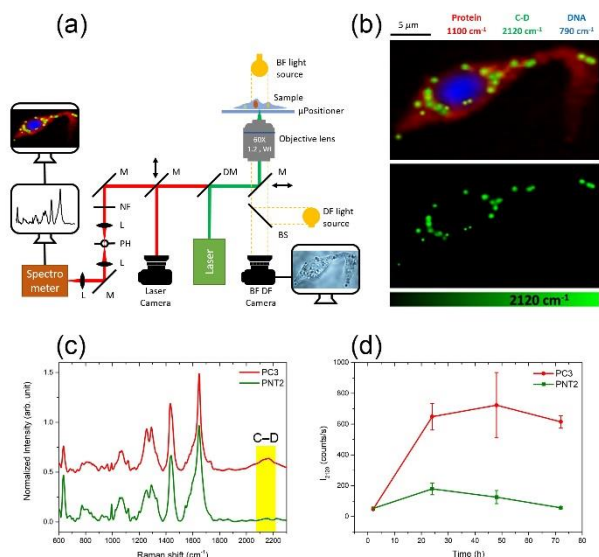


**Fig. 1.** (a) Raman imaging setup, (b) Raman image of PC3 cell, (c) Raman spectra of PC3 and PNT2 cells, (d) dynamics of intensity of C–D band for different incubation times.

Given these morphological characteristics, it can be inferred that these points are lipid droplets. Therefore, all glucose uptake by cells is accumulated as fatty acids and cholesteryl esters in lipid droplets. Figure 1(c) illustrates Raman spectra for lipid droplets of PNT2 and PC3 cells. The intensity of the  $2120\text{ cm}^{-1}$  peak in cancer cells is much higher than in healthy cells. Figure 1(d) depicts the intensity of this peak for different incubation times with significant difference at 48 h. However, considering that the acquisition time for each point is 1 seconds, this method may not be suitable for screening purposes.

Figure 2 illustrates the resultant image of PSDHI. As evident, there are circular regions in the peripheral regions within the cell that have a high degree of birefringence. These points are not only geometrically very similar to lipid droplets, but spatially there is a high agreement between the location of these points and the location of lipid droplets obtained in Raman imaging in Figure 1. Therefore, it can be concluded that these particles are lipid droplets. Figure 3 presents the results of discrimination parameters by applying principal component analysis (PCA) on data obtained from Raman spectroscopy and PSDHI for various incubation times. The results of

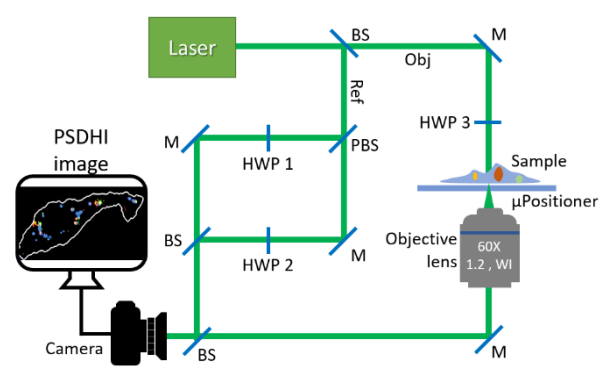


**Fig. 2.** Experimental optical setup for polarization-sensitive digital holography imaging.

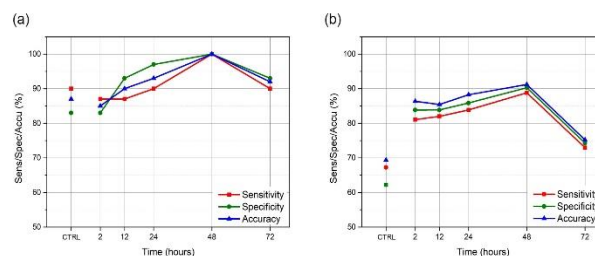


**Fig. 3.** Sensitivity, specificity, and accuracy of (a) Raman spectroscopy, and (b) PSDHI for different incubation times.

PSDHI show very good agreement with Raman spectroscopy results. Almost all discrimination parameters for PSDHI are above 80% and reach around 90% at a 48-hour incubation time, indicating that PSDHI has a high capability in distinguishing cancer cells from healthy ones but at a much faster rate compared to RM.

## 4 Conclusion

In this study, we utilized two non-destructive optical techniques, Raman microscopy and PSDHI, for the detection of prostate cancer cells. While Raman spectroscopy demonstrated a nearly 100% performance in detecting prostate cancer cells, its time-consuming nature renders it less suitable for screening purposes. PSDHI, as a rapid method based on the birefringence of lipid droplets, yielded results closely comparable to Raman microscopy and indicated its potential as a rapid and non-destructive method for the detection of prostate cancer cells.

## Acknowledgement

This work was financially supported by the Italian Association for Cancer Research (AIRC IG Grant 21420), Campania Region (POR Campania FESR 2014–2020 PLATT and Ciro).

## References

1. R. L. Siegel, K. D. Miller, N. S. Wagle, and A. Jemal, *CA Cancer J Clin* **73**, 17 (2023).
2. H. B. Carter, P. C. Albertsen, M. J. Barry, R. Etzioni, S. J. Freedland, K. L. Greene, L. Holmberg, P. Kantoff, B. R. Konety, M. H. Murad, D. F. Penson, and A. L. Zietman, *Journal of Urology* **190**, 419 (2013).
3. S. Elumalai, S. Managò, and A. C. De Luca, *Sensors* **20**, (2020).
4. M. Mangini, M. A. Ferrara, G. Zito, S. Managò, A. Luini, A. C. De Luca, and G. Coppola, *Front Bioeng Biotechnol* **11**, (2023).
5. Y. Park, C. Depeursinge, and G. Popescu, *Nat Photonics* **12**, 578 (2018).
6. M. A. Ferrara, G. Di Caprio, S. Managò, A. De Angelis, L. Sirlito, G. Coppola, and A. C. De Luca, *Biosensors (Basel)* **5**, 141 (2015).
7. O. Warburg, *Science* (1979) **124**, 269 (1956).
8. J. Li and J.-X. Cheng, *Sci Rep* **4**, 6807 (2014).